Applied Physics Letters

The microcontainer shape in electropolymerization on bubbles

Cite as: Appl. Phys. Lett. **94**, 034103 (2009); https://doi.org/10.1063/1.3073861
Submitted: 03 September 2008 . Accepted: 01 January 2009 . Published Online: 23 January 2009

J. T. Kim, S. K. Seol, J. H. Je, Y. Hwu, and G. Margaritondo

View Online

Export Citation

ARTICLES YOU MAY BE INTERESTED IN

Hard-x-ray microscopy with Fresnel zone plates reaches $40\mathrm{nm}$ Rayleigh resolution
Applied Physics Letters **92**, 103119 (2008); https://doi.org/10.1063/1.2857476

Template-free synthesis of conducting-polymer polypyrrole micro/nanostructures using electrochemistry
Applied Physics Letters **88**, 063108 (2006); https://doi.org/10.1063/1.2168688

Lock-in Amplifiers up to 600 MHz
Watch

AIP Publishing

© 2009 American Institute of Physics.

The microcontainer shape in electropolymerization on bubbles

J. T. Kim,[1] S. K. Seol,[1,a)] J. H. Je,[1,b)] Y. Hwu,[2] and G. Margaritondo[3]
[1]*Department of Materials Science and Engineering, X-ray Imaging Center (XIC), Pohang University of Science and Technology, Pohang 790784, Republic of Korea*
[2]*Institute of Physics, Academia Sinica, 128 Academia Rd., Sec.2, Nankang, Taipei 11529, Taiwan*
[3]*Faculté des Sciences de Base, Ecole Polytechnique Fédérale, CH-1015 Lausanne, Switzerland*

(Received 3 September 2008; accepted 1 January 2009; published online 23 January 2009)

We investigated the microcontainer shape in electropolymerization of polypyrrole (PPy) on bubbles using real-time microradiography. We revealed the existence of a "deformation force" at the three-phase boundary among gas (bubble), liquid (electrolyte), and solid (PPy). As the deformation force increases, the microcontainer shape gradually changes from spherical to elliptical and then to cylindrical. The force is proportional to the polymerization rate that is enhanced by the applied voltage and monomer concentration. © *2009 American Institute of Physics*.
[DOI: 10.1063/1.3073861]

Micro- and nanostructures of conducting polymers are increasingly important in modern technology. They have a variety of applications in electronics,[1] photonics,[2] and biomedical science[3] because of their electrical and optical properties similar to metals or semiconductors with the advantage of flexibility, easy processing, and biocompatibility.[4] Several types of the micro- and nanostructures such as particles,[5] wires,[4] and thin films[6] were fabricated for diverse applications. In particular, microcontainers of conducting polymers,[7–10] because of their structural properties such as low density and large surface area, are suitable for sensors, catalysts, microreactors, and drug delivery systems.

In general, microcontainers are fabricated with the hard template method, a coating process on template particles (e.g., polystyrene and silica beads).[7,8] This method yields well-defined shapes but involves complicated and expensive procedures to synthesize the templates. In addition, the post-deposition template removal decreases the production yield.

Recently, a template-free approach was proposed to eliminate the above problems.[9,10] H_2 bubbles produced by the electrolysis of water are used as templates instead of hard particles. This method offers easy formation and removal of the bubble templates but has limited control of the microcontainer shape, essential for many applications such as drug delivery[11,12] and highly sensitive sensors.[13]

We investigated the shape of polypyrrole (PPy) microcontainers fabricated with the bubble template approach using real-time microradiography with coherent x rays.[14–17] The most relevant result for application was the detection of a "deformation force" at the three-phase boundary among gas (bubble), liquid (electrolyte), and solid (PPy). In fact, by increasing the polymerization rate, the said force increases, inducing a shape change from spherical to elliptical and then to cylindrical.

The fabrication of PPy microcontainers by polymerization on H_2 bubbles was implemented at room temperature using $0.05M-0.5M$ pyrrole and $0.5M$ 2-naphthalenesulfonic acid (β-NSA) in aqueous solution. Platinum-coated silicon wafers placed 0.5 cm apart were used as electrodes. The microradiology observations were performed at the "7B2 X-ray Microscopy" beamline of the Pohang Light Source (PLS), Korea,[18] in a specially designed miniature solution bath machined from a Teflon block and sealed with Kapton films that were x-ray transparent and stable for most chemical reaction. The distance between the two cell windows was optimized to ~5 mm to avoid unnecessary x-ray absorption by the electrolyte. Field emission scanning electron microscopy (FE-SEM) (JEOL JSM6330F) was used to study the microscopic characteristics of the grown structures. For FE-SEM, the sample was cleaned using de-ionized water.

Figure 1 shows a series of real-time microradiographs, illustrating the PPy electropolymerization on a H_2 bubble with $0.5M$ pyrrole. Quite remarkably, microradiography with coherent x rays enabled us to visualize not only the bubble but also the electropolymerized PPy on it. Figure 1(a) shows the H_2 bubble generated by the electrolysis of water on the working electrode with a negative bias of −1.0 V. Real-time

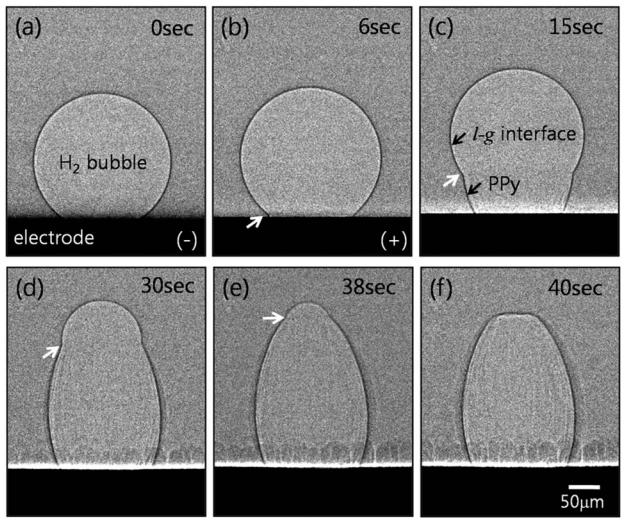

FIG. 1. Real-time coherent x-ray microradiographs showing the PPy electropolymerization on a H_2 bubble in a $0.5M$ pyrrole and $0.5M$ β-NSA aqueous solution. (a) Hydrogen bubble formed by decomposition of water on the working electrode negatively biased at −1.0 V. [(b)–(f)] Electropolymerization on the bubble for a 2.5 V positive bias at (b) 6 s, (c) 15 s, (d) 30 s, (e) 38 s, and (f) 40 s. Note that the bubble is constrained at the three-phase boundary (white arrow) among the gas, the liquid, and the PPy solid.

a)Present address: Center for Pioneering Medical-Physics Research, Korea Electrotechnology Research Institute (KERI), Ansan-city 426-170, Korea.
b)Electronic mail: jhje@postech.ac.kr.

 © 2009 American Institute of Physics

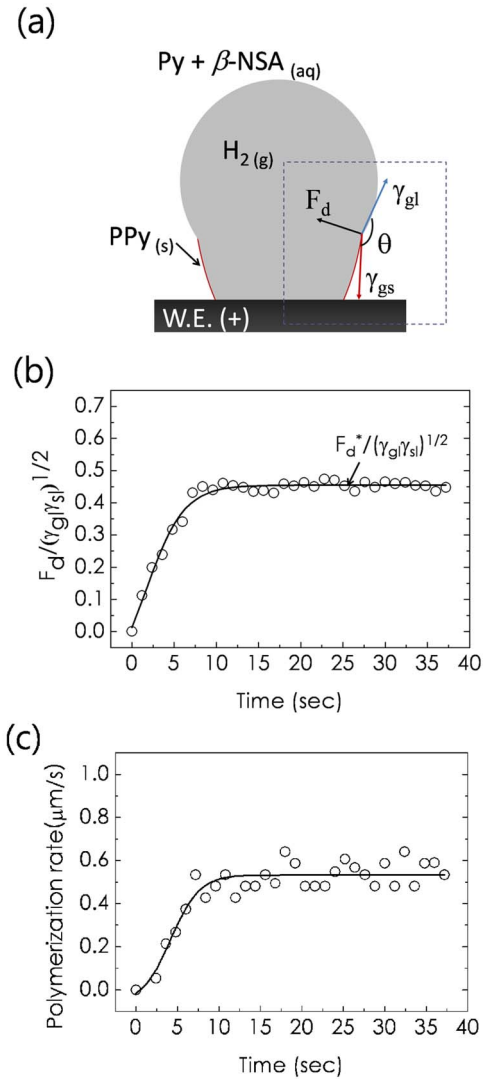

FIG. 2. (Color online) (a) Schematic diagram of the force balance among F_d, γ_{gl}, and γ_{gs} at the three-phase boundary for the grown structure in Fig. 1(c). (b) Plot of $F_d/(\gamma_{gl}\gamma_{gs})^{1/2}$ as a function of the growth time. (c) Plot of the polymerization rate as a function of the growth time. The changes in the deformation force match those of the polymerization rate, suggesting a linear relation between these two quantities.

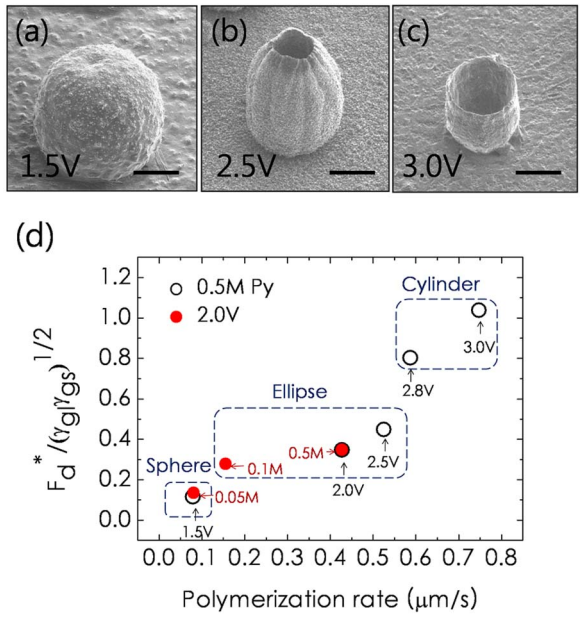

FIG. 3. (Color online) FE-SEM images of PPy structures grown with a bias of (a) 1.5 V (sphere), (b) 2.5 V (ellipse), and (c) 3.0 V (cylinder) [scale bar: 50 μm]. (d) Plot of $F_d^*/(\gamma_{gl}\gamma_{gs})^{1/2}$ as a function of the polymerization rate that is controlled by changing the applied voltage (open circles) in 0.5*M* pyrrole or by changing the monomer concentration (closed dots) with a bias of 2.0 V.

microradiography enabled us to accurately control the bubble size; for example, ~200 μm bubbles were obtained by applying the negative potential to the working electrode for 3 s [Fig. 1(a)]. Then, PPy electropolymerization was obtained with a positive 2.5 V bias as shown in Figs. 1(b)–1(f). The continuous growth of PPy on the bubble can be detected from the wrinkled bubble surface (the columnar structures on the working electrode are from the PPy film directly deposited on it and not related to the microcontainer). The bottom part of the PPy structure, which is connected to the electrode, is, however, open at the bottom side.

The shape of the PPy structure, initially growing on the spherical bubble, gradually deviates from the sphericity finally changing to elliptical while the liquid-gas interface remains spherical. The curvature of the liquid-gas interface continuously increases during the PPy growth. The flat top of the grown PPy structure in Fig. 1(f) is due to the bubble shrinkage caused by the enhanced Laplace pressure on the top liquid-gas interface region with a high curvature [Fig. 1(e)] in the late stages of the process.[19] Interestingly, the bubble is constrained at the three-phase boundary (white arrow) among the gas, the liquid, and the PPy solid.

In order to understand the phenomena and in particular the shape changes, we considered the force balance [illustrated in Fig. 2(a)] for the grown structure in Fig. 1(c). We derived the existence of a deformation force F_d countering the gas-liquid and the gas-solid surface tensions γ_{gl} and γ_{gs} that causes the bubble to deform at the three-phase boundary

$$F_d = (\gamma_{gl}^2 + \gamma_{gs}^2 + 2\gamma_{gl}\gamma_{gs}\cos\theta)^{1/2}. \quad (1)$$

Assuming $\gamma_{gl} \approx \gamma_{gs}$,[20,21] the deformation force can be simply derived from θ,

$$F_d/(\gamma_{gl}\gamma_{gs})^{1/2} \sim (2 + 2\cos\theta)^{1/2}. \quad (2)$$

The θ values measured from the images in Fig. 1 yielded the deformation force plotted as a function of the growth time in Fig. 2(b). After an initial gradual increase, the force saturates to a constant value F_d^* (the force balance disappears in the last stage of growth (>38 s) due to the bubble shrinkage [Fig. 1(f)]). Note that the evolution of the deformation force matches well with that of the polymerization rate [Fig. 2(c)], estimated by measuring the thickness of the grown structure in the images in Fig. 1. This indicates that the deformation force is proportional to the polymerization rate. The initial increase in the polymerization rate due to a charge transfer reaction induces the initial increase in the deformation force, which in turn corresponds to the gradual shape change from spherical to elliptical. An elliptical shape is maintained during the saturation period, corresponding to a constant polymerization rate due to a diffusion-controlled reaction.[22]

These experimental observations led us to a method for controlling the shape of the grown PPy structure by tuning the deformation force. Because of its proportionality to the polymerization rate, the force can be changed by adjusting electrochemical parameters such as the applied voltage and

the monomer concentration. Indeed the shape of the grown structure changes from spherical [Fig. 3(a)] to elliptical [Fig. 3(b)] and then to cylindrical [Fig. 3(c)] as the bias increases from 1.5 to 2.5 and then to 3.0 V for 0.5*M* pyrrole. These shape changes can be explained by the increase in the deformation force with bias. Figure 3(d) shows that the increases in the bias or in the monomer concentration augment the polymerization rate and the deformation force.

In summary, we conceived and tested a simple but effective approach to modulate the shape of microcontainers fabricated on bubbles by electropolymerization. This approach can be implemented for many other cases of template-free fabrication.

This work was supported by the Creative Research Initiatives (Functional X-ray Imaging) of MEST/KOSEF.

[1]A. G. MacDiarmid, Angew. Chem., Int. Ed. **40**, 2581 (2001).
[2]R. H. Friend, R. W. Gymer, A. B. Holmes, J. H. Burroughes, R. N. Marks, C. Taliani, D. D. C. Bradley, D. A. Dos Santos, J. L. Brédas, M. Lögdlund, and W. R. Salaneck, Nature (London) **397**, 121 (1999).
[3]C. E. Schmidt, V. R. Shastri, J. P. Vacanti, and R. Langer, Proc. Natl. Acad. Sci. U.S.A. **94**, 8948 (1997).
[4]K. Ramanathan, M. A. Banger, M. Yun, W. Chen, A. Mulchandani, and N. V. Myung, Nano Lett. **4**, 1237 (2004).
[5]J. Jang, J. H. Oh, and G. D. Stucky, Angew. Chem., Int. Ed. **41**, 4016 (2002).
[6]M. Halik, H. Klauk, U. Zschieschang, T. Kriem, G. Schmid, and W. Radlik, Appl. Phys. Lett. **81**, 289 (2002).
[7]S. M. Marinakos, J. P. Novak, L. C. Brousseau, A. B. House, E. M. Edeki, J. C. Feldhaus, and D. L. Feldheim, J. Am. Chem. Soc. **121**, 8518 (1999).
[8]Y. Lu, Y. Yin, and Y. Xia, Adv. Mater. (Weinheim, Ger.) **13**, 271 (2001).
[9]S. Gupta, Appl. Phys. Lett. **88**, 063108 (2006).
[10]V. Bajpai, P. He, and L. Dai, Adv. Funct. Mater. **14**, 145 (2004).
[11]S. L. Tao and T. A. Desai, Adv. Mater. (Weinheim, Ger.) **17**, 1625 (2005).
[12]Y. Zhou and X. Y. Wu, J. Controlled Release **49**, 277 (1997).
[13]M. Ma, L. Qu, and G. Shi, J. Appl. Polym. Sci. **98**, 2550 (2005).
[14]W. L. Tsai, P. C. Hsu, Y. Hwu, C. H. Chen, L. W. Chang, J. H. Je, H. M. Lin, A. Groso, and G. Margaritondo, Nature (London) **417**, 139 (2002).
[15]Y. Hwu, W. L. Tsai, A. Groso, G. Margaritondo, and J. H. Je, J. Phys. D **35**, R105 (2002).
[16]S. K. Seol, A. R. Pyun, Y. Hwu, G. Margaritondo, and J. H. Je, Adv. Funct. Mater. **15**, 934 (2005).
[17]S. K. Seol, J. T. Kim, J. H. Je, Y. Hwu, and G. Margaritondo, Macromolecules **41**, 3071 (2008).
[18]S. Baik, H. S. Kim, M. H. Jeong, C. S. Lee, J. H. Je, Y. Hwu, and G. Margaritondo, Rev. Sci. Instrum. **75**, 4355 (2004).
[19]E. G. Schutt, D. H. Klein, R. M. Mattrey, and J. G. Riess, Angew. Chem., Int. Ed. **42**, 3218 (2003).
[20]M. M. Chehimi, M. Abel, C. Perruchot, M. Delamar, S. F. Lascelles, and S. P. Armes, Synth. Met. **104**, 51 (1999).
[21]I. Díez, K. Tauer, and B. Schulz, Colloid Polym. Sci. **283**, 125 (2004).
[22]Y. Li, J. Electroanal. Chem. **433**, 181 (1997).